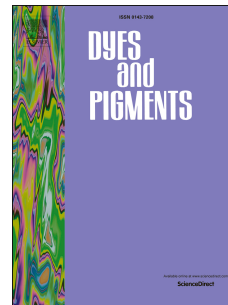


Accepted Manuscript

Turn on fluorescent detection of hydrazine with a 1,8-naphthalimide derivative

Bingjie Shi, Yangyang He, Panpan Zhang, Yulong Wang, Mingming Yu, Hongyan Zhang, Liuhe Wei, Zhanxian Li



PII: S0143-7208(17)31185-3

DOI: [10.1016/j.dyepig.2017.08.010](https://doi.org/10.1016/j.dyepig.2017.08.010)

Reference: DYPI 6172

To appear in: *Dyes and Pigments*

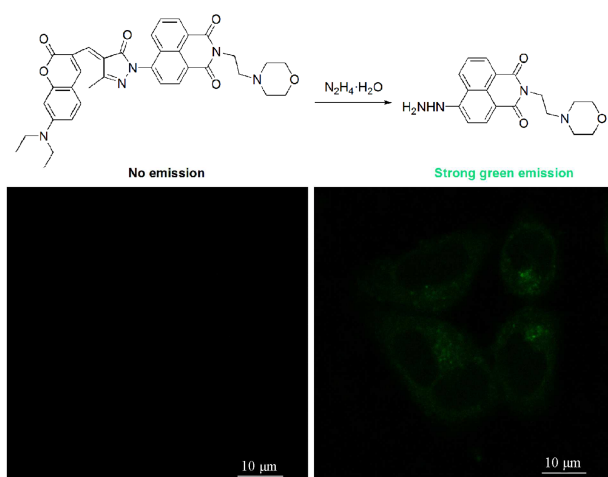
Received Date: 22 May 2017

Revised Date: 24 July 2017

Accepted Date: 9 August 2017

Please cite this article as: Shi B, He Y, Zhang P, Wang Y, Yu M, Zhang H, Wei L, Li Z, Turn on fluorescent detection of hydrazine with a 1,8-naphthalimide derivative, *Dyes and Pigments* (2017), doi: 10.1016/j.dyepig.2017.08.010.

This is a PDF file of an unedited manuscript that has been accepted for publication. As a service to our customers we are providing this early version of the manuscript. The manuscript will undergo copyediting, typesetting, and review of the resulting proof before it is published in its final form. Please note that during the production process errors may be discovered which could affect the content, and all legal disclaimers that apply to the journal pertain.



ACCEPTED MANUSCRIPT

Turn on fluorescent detection of hydrazine with a 1,8-naphthalimide derivative

Bingjie Shi^a, Yangyang He^a, Panpan Zhang^b, Yulong Wang^a, Mingming Yu^{*a}, Hongyan Zhang^{*c}, Liuhe Wei^a, Zhanxian Li^{*a}

* Corresponding author.

a. College of Chemistry and Molecular Engineering, Zhengzhou University, Zhengzhou, 450001, China.

E-mail address: yummm@zzu.edu.cn (M. Yu), lizx@zzu.edu.cn (Z. Li).

Tel: +(86)371-67781205

Fax: +(86)371-67781205

b. Institute of Functional Nano & Soft Materials (FUNSOM), Collaborative Innovation Center of Suzhou Nano Science and Technology, Jiangsu Key Laboratory for Carbon-Based Functional Materials & Devices, Soochow University, Suzhou 215123, China

c. Key Laboratory of Photochemical Conversion and Optoelectronic Materials, Technical Institute of Physics and Chemistry, Chinese Academy of Sciences, Beijing, 100190, China

E-mail address: zhanghongyan@mail.ipc.ac.cn (H. Zhang).

Abstract

It is crucial to develop highly sensitive and selective probes toward hydrazine because it is a class of highly toxic and pollutant compound. Herein, using fracture of carbon carbon double bond and dissociation of amide by hydrazine, a novel off-on fluorescent probe was developed for hydrazine. The probe can quantitatively detect hydrazine in concentration range from 0 to 20 μM with the LOD of 140 nM. Further, it displayed excellent selectivity and anti-interference ability over many neutral molecules, metal ions, anions, and biological species. The ability to target lysosome and the response of hydrazine to this probe in a living cell was successfully tracked via fluorescence imaging.

Keywords: Fluorescent probe; Off-on; 1,8-Naphthalimide; Hydrazine; Fluorescence imaging.

1. Introduction

Hydrazine is widely used not only in the pharmaceutical, chemical and agricultural industries, but also in rocket-propulsion and missile systems [1–4]. On the other hand, as a class of highly toxic and pollutant compound, hydrazine can potentially lead to serious environmental contamination during its manufacture, use, transport and disposal. In addition, as a neurotoxin, hydrazine has several mutagenic effects, which can cause damage to the liver, lungs, kidneys and human central nervous system [5–9]. Therefore, it is urgently necessary to develop an efficient and simple method for determining hydrazine level in both environmental and biological science.

Some approaches such as chromatography-mass spectrometry [10–12], titration [13] and electrochemical methods [14–18] have been reported to measure hydrazine, but their shortcomings such as complicated equipment, sample handling and professional operating will limit their application. Therefore, it is difficult to detect trace hydrazine in situ, with short time and low cost in room temperature. On the other hand, fluorescence-based method has been widely used to detect various analytes such as metal ions, anions and biomolecules due to its simplicity, high sensitivity, rapid response, and capacity of real-time and in situ monitoring of the dynamic biological processes in living cells [19–29]. However, available fluorescent probes for hydrazine are still very limited [30–40]. Hence, it is needed to develop fluorescent probes toward hydrazine.

In this paper, using hydrazine-induced fracture of C=C and amide bonds, a highly sensitive fluorescent off-on probe **1** was developed (Scheme 1), and the application of which for selective detection and imaging of hydrazine in living cells was successfully demonstrated. The probe exhibited a high sensitivity (the LOD is 140 nM), a wide linear response range from hydrazine concentration of 0-20 μM , excellent selectivity and

anti-interference ability against other various species.

2. Experimental

2.1. Methods and materials

All commercial grade chemicals and solvents were purchased and used without further purification.

Mass spectra were obtained on high resolution mass spectrometer (IonSpec4.7 Tesla FTMS-MALDI/DHB). ^1H and ^{13}C NMR spectra were recorded on a Bruker 400 NMR spectrometer. Chemical shifts are reported in parts per million using tetramethylsilane (TMS) as the internal standard.

2.2. Spectral characterizations

All spectral characterizations were carried out in HPLC-grade solvents at 20°C within a 10 mm quartz cell. UV-vis absorption spectra were measured with a TU-1901 double-beam UV-vis spectrophotometer. Fluorescence spectra were determined on a Hitachi F-4600 spectrometer.

2.3. Cell viability assay

The dark toxicity (The survival rate of cells which have been incubated with certain probe for 1 hour without excitation light.) of the material: the stock solutions were diluted with fresh medium to various concentrations (5, 10, 15 and 20 μM). The cell medium was then exchanged for different concentrations of material medium solution. The cells were then incubated with these solutions at 37 °C in 5% CO_2 for 1 h before removing the material solution and adding fresh medium. Subsequently, the plates were incubated at 37 °C in 5% CO_2 for 24 h. The cell medium solutions were exchanged for 100 μL of fresh medium, followed by the addition of 20 μL of MTT solution to each well. The culture

plates were then incubated at 37 °C in 5% CO₂ for 4 h. The culture medium was discarded, and 100 µL of dimethylsulfoxide was added. The absorbance of an untreated cell population under the same experimental conditions was used as the reference point to establish 100% cell viability. The ratiometric confocal fluorescence images are recorded by a Nikon A1 RSiMP Confocal Microscopy with a 60 ×WI objective (NA 1.27) and 457 nm diode laser.

2.4. Cell incubation and imaging

The HeLa cells were incubated with the synthesized probe at 37°C for fluorescence imaging with Nikon A1Rmp Confocal microscopy. The fluorescent images were recorded at green with 500-550 nm filters after the cells incubated with probe (10⁻⁵ M) for 30 min. After adding 1.0 × 10⁻⁴ M hydrazine and incubation for 1 h, the fluorescent images were taken at the same situation. The fluorescence excitation was performed at 457 nm using a diode laser with pin hole and 60x oil objective lens.

2.5. Synthesis of compound 7

(Insert: Scheme 1)

4-Diethylaminosalicylaldehyde (0.4827 g, 2.5 mmol), diethylmalonate (750 µL, 5 mmol) and piperidine (250 µL) were combined in absolute ethanol (15 mL) and stirred for 6 hours under refluxing conditions. Ethanol was evaporated under reduced pressure, and then concentrated HCl (10 mL) and glacial acetic acid (10 mL) were added to hydrolyze the reaction with stirring for another 6 hours. The solution was cooled to room temperature and poured into 15 mL ice water. NaOH solution (40%) was added dropwise to modulate pH of the solution to 5, and a pale precipitate was formed immediately. After stirring for 30 min, the mixture was filtered, washed with water, and then the final product was purified by silica gel column chromatography using DCM/ethanol (1/100 v/v)

as eluent with a yield of 48% (Scheme 1). ^1H NMR (400 MHz, CDCl_3-d_6 , TMS): δ_{H} 7.54 (d, 1H), 7.27 (t, 1H), 6.50 (d, 1H), 6.50 (m, 1H), 6.03 (d, 1H), 3.42 (m, 4H), 1.24 (t, 6H). ^{13}C NMR (100 MHz, CDCl_3-d_6): δ_{C} 162.28, 156.74, 150.66, 143.70, 128.77, 109.19, 108.67, 108.29, 97.53, 44.82, 12.44.

2.6. Synthesis of compound 2

Fresh distilled DMF (1 mL) was added dropwise to POCl_3 (1 mL) at 20-50 °C within N_2 atmosphere and stirred for 30 minutes to yield a red solution. This solution was combined with a portion of **7** (0.2543 g, 1.2 mmol, dissolved in 2 mL DMF) to yield a scarlet suspension. The mixture was stirred at 60 °C for 12 hours and then poured into 15 mL of ice water. NaOH solution (20%) was added to adjust the pH of the mixture to yield a large amount of precipitate. The crude product was filtered, thoroughly washed with water, dried and then the final product was purified by silica gel column chromatography using DCM as eluent with a yield of 58.5%. ^1H NMR (400 MHz, CDCl_3-d_6 , TMS): δ_{H} 10.13 (s, 1H), 8.26 (s, 1H), 7.43 (d, 1H), 6.67 (m, 1H), 6.51 (d, 1H), 3.50 (m, 4H), 1.27 (t, 6H). ^{13}C NMR (100 MHz, CDCl_3-d_6): δ_{C} 187.92, 161.89, 158.93, 153.47, 145.37, 132.52, 110.20, 108.23, 97.15, 45.29, 29.70, 12.46.

2.7. Synthesis of compound 5

4-bromo-1,8-naphthalic anhydride (1.0002 g, 3.6 mmol) and 4-(2-aminoethyl)-morpholine (945 μL , 7.2 mmol) were dissolved in 40 mL ethanol, and the solution was refluxed for 2 hours. After cooling to room temperature, the yellowish sediments were collected by filtration and then dried overnight at room temperature in a vacuum oven to obtain **5** (1.3611 g, 3.5 mmol, yield: 97.2%). ^1H NMR (400 MHz, $\text{DMSO}-d_6$, TMS): δ_{H} 8.85 (m, 1H), 8.57 (m, 1H), 8.41 (m, 1H), 8.05 (m, 1H), 7.86 (m, 1H), 4.37 (t, 2H), 3.70 (t, 4H), 2.72 (t, 2H), 2.62 (s, 4H). ^{13}C NMR (100 MHz, $\text{DMSO}-d_6$):

δ_c 163.62, 163.60, 133.31, 132.04, 131.23, 131.12, 130.64, 130.32, 129.03, 128.10, 123.05, 122.18, 67.02, 56.09, 53.81, 37.30.

2.8. Synthesis of compound **4**

A mixture of compound **5** (1.0113 g, 2.6 mmol), (3030 μ L, 13 mmol) 80% hydrazine hydrate and 15 mL 2-Methoxyethanol were refluxed for 8 h. After cooling to room temperature, some of the 2-Methoxyethanol was evaporated under reduced pressure, and then massive ether was added. The orange solid product was obtained by filtration and being washed with ether three times with a yield of 92.3%. HRMS (EI) m/z: $C_{18}H_{20}N_4O_3$ [M+H], 341.1535, found, 341.1612.

2.9. Synthesis of compound **3**

Compound **4** (0.3403 g, 1 mmol) and ethyl acetoacetate (255 μ L, 2mmol) were dissolved in 16 mL ethanol, and the solution was refluxed for 8 hours. The reaction solution was then cooled to room temperature. The crude product **3** was purified by silica gel column chromatography using acetic ether as eluent. The yield was 75%. This product was used without characterization.

2.10. Synthesis of compound **1**

Compound **3** (0.1681 g, 0.69 mmol), and compound **2** (0.1681 g, 0.69 mmol) were mixed in absolute alcohol (10 mL). Triethylamine (50 μ L, 1.7 mmol) was added to it and stirred at room temperature for 30 min. After refluxing for 20 h, the mixture solution was then allowed to cool to room temperature and stirred for 5 h at room temperature. The purple solid was filtered and washed with ethanol. The final product was obtained by vacuum drying at 25 °C for 12 h (0.1823 g, 0.28 mmol, 41%). HRMS (EI) m/z: $C_{36}H_{35}N_5O_6$ [M+H], 634.2587; found, 634.2612. Elemental analysis data: C (68.23%), H

(5.57%), N (11.05%); found C (67.96%), H (5.59%), N (11.01%). ^1H NMR (400 MHz, CDCl_3 - d_6 , TMS): δ_{H} 10.39 (d, 1H), 8.68 (m, 2H), 8.50 (m, 1H), 8.07 (m, 1H), 7.93 (m, 1H), 7.82 (m, 1H), 7.46 (m, 1H), 6.66 (m, 1H), 6.64 (m, 1H), 4.39 (d, 2H), 3.7 (s, 4H), 3.5 (m, 4H), 2.75(s, 2H), 2.63(s, 4H), 2.45(s, 3H), 1.29(t, 6H). ^{13}C NMR (100 MHz, CDCl_3 - d_6): δ_{C} 164.21, 164.13, 163.73, 161.98, 158.71, 153.90, 152.85, 150.30, 142.30, 139.90, 133.14, 131.62, 131.51, 131.22, 127.10, 126.85, 123.83, 123.05, 121.45, 112.52, 110.49, 109.62, 97.20, 67.09, 56.09, 53.83, 45.45, 37.28.

3. Results and Discussion

3.1. Synthesis of probe **1**

The synthesis of the smart probe **1** was accomplished in four steps as shown in Scheme 1 [41–44]. The starting materials 4-bromo-1,8-naphthalic anhydride and morpholine were reacted in ethanol for 2 hours under 80°C to give compound **5** in a yield of 97.2%. The product **5** and hydrazine hydrate reacted in ethylene glycol monomethyl ether to give product **4** in a yield of 92.5%. Compound **4** reacted with ethyl acetoacetate in ethanol for 8 h to give compound **3** in a yield of 75.0%. Probe **1** was obtained by the reaction of compounds **3** and **2** in a yield of 41%. The detailed synthetic procedures are presented in the Experimental section. All new compounds were carefully characterized by ^1H NMR, ^{13}C NMR and HRMS in supporting information.

(Insert: Fig. 1)

3.2. Hydrazine recognition properties of **1**

To study the recognition properties of probe **1** toward hydrazine, fluorescence titration experiments (Figures **1a** and **1b**) were conducted with 0.1 M hydrazine in aqueous solution of **1** (the molar extinction coefficient is $7.46 \times 10^4 \text{ M}^{-1}\text{cm}^{-1}$, $1.0 \times 10^{-5} \text{ M}$,

$V_{\text{HEPES}}:V_{\text{DMSO}} = 4:6$, pH = 7.40). Upon excitation at 440 nm, the characteristic emission band of 1,8-naphthalic anhydride centered at 517 nm underwent an increase of about 24 times (the fluorescent quantum yield changed from 1.04% to 10.5%) as the concentration of hydrazine increased from 0 to 10 equiv. As demonstrated in Fig. 1b, in the concentration range of 0-20 μM , the fluorescence intensity at 517 nm were in good linear relationship with hydrazine concentration, implying that hydrazine can be quantitatively detected in a wide concentration range in fluorescence mode. From the linear calibration graph with the fluorescence titration experiment (**Fig. 1b**), the detection limit of probe **1** for hydrazine was figured out to be about 140 nM based on signal-to-noise ratio (S/N) = 3 [45–47], which is much lower than the threshold limit value of hydrazine permitted for human health (312 nM). These results led us to conclude that probe **1** could be an effective off-on fluorescent probe for hydrazine.

hydrazine in time-dependent fluorescence spectra of probe **1** hydrazine is completely accomplished within 1 h and hydrazine can be detected within 8 min when the concentration of hydrazine is higher or equal to 8.0×10^{-6} M. Such result further proved the fast response and high sensitivity of **1** for detection of hydrazine.

3.3. pH range in application of probe **1** toward hydrazine

The pH value of solution was found to be essential to the reaction between probe **1** and hydrazine. To investigate the pH effect, the fluorescence of 10.0 μM probe **1** in the absence and presence of 100 μM hydrazine were examined at pH range from 4.0 to 10.0. As shown in **Fig.1d**, probe **1** itself is stable and its emission spectra are not changed in a wide pH range from 4.0 to 10.0. Although there was a significant fluorescence change of probe **1** in pH ranges from 4.0 to 10.0 upon addition of hydrazine. Probe **1** is able to detect hydrazine in a relatively wide pH range.

3.4. Recognition mechanism of probe **1** toward hydrazine

The recognition mechanism was studied by Mass spectrometry. For pure probe **1**, a characteristic peak at $m/z = 634.2665$ was obtained which corresponds to the specie **1** [$M + H$], whilst after reaction with hydrazine, the peak at 634.2665 disappeared and two new peaks appeared at $m/z = 341.1514$ and 242.3710 , which are corresponding to compounds **4** ($M + H$) and **6** ($M + H$) indicating the decomposition of probe **1** and the formation of new compounds **4** and **6** (Scheme 1). To further clarify the recognition mechanism, we have separated one product from the reaction of probe **1** and hydrazine hydrate, which has the same R_f value as that of compound **6**. In addition, we have also measured the fluorescence quantum yields of probe **1** (1.04%), the reaction solution of probe **1** and hydrazine hydrate (10.5%), compound **4** (2.51%), and compound **6** (19.4%) (Scheme 1), indicating that the fluorescence mainly comes from compound **6** upon addition of hydrazine hydrate into the solution of probe **1**. Besides, we have also characterized the product from the reaction of probe **1** and hydrazine hydrate with HRMS, ^1H NMR, and ^{13}C NMR. Characterization data were as follows: HRMS (EI) m/z : $\text{C}_{14}\text{H}_{15}\text{N}_3\text{O}$ [$M+H$], 242.1293; found, 242.3710. ^1H NMR (400 MHz, CDCl_3-d_6 , TMS): δ_{H} 11.82 (s, 1H), 8.47 (s, 1H), 7.12 (s, 1H), 6.27 (t, 2H), 3.42 (q, 4H), 1.23 (t, 6H). ^{13}C NMR (100 MHz, CDCl_3-d_6): δ_{C} 161.45, 160.91, 151.21, 133.28, 106.95, 103.97, 97.87, 44.57, 29.71, 12.71.

(Insert: Fig. 2)

3.5. The selectivity of **1** for hydrazine

To evaluate the selectivity of probe **1** for hydrazine, various species including neutral molecules including Et_3N , $\text{NH}_3 \cdot \text{H}_2\text{O}$, $\text{C}_2\text{H}_4(\text{NH}_2)_2$, thiourea, urea, and aniline, metal ions (Na^+ , Mg^{2+} , Al^{3+} , K^+ , Ca^{2+} , Cr^{3+} , Mn^{2+} , Zn^{2+} , Pt^{2+} , and Pb^{2+}), anions (HPO_4^{2-} , H_2PO_4^- , PO_4^{3-} , N_3^- , HSO_3^- , $\text{P}_2\text{O}_7^{4-}$, CO_3^{2-} , $\text{C}_2\text{O}_4^{2-}$, SiO_3^{2-} , Cl^- , F^- , NO_3^- , SO_3^{2-} , $\text{S}_2\text{O}_3^{2-}$, ClO_3^- , I^- ,

SO_4^{2-} , CH_3COO^- , and HS^-), and nucleophilic biological species (Gly, Gin, GSH, Asp, Cys, Thr, Ala, Phe, Met, Lys, Leu, Ile, Val, Glu, Ser, Arg, Pro, Hcy and Tyr) were tested. As shown in Figures **S1**, **S2**, **S3** and **S4** in supporting information and red bars of Figures **2** and **3**, only hydrazine induced a significant fluorescence change, whilst, other tested species did not induce any obvious fluorescence change, indicating the good selectivity of probe **1** toward hydrazine.

3.6. The anti-disturbance effect of 1 for hydrazine detection

To further assess its utility as a hydrazine-selective fluorescent probe, its fluorescent response to hydrazine in complicated surroundings as mentioned above was also tested (figures **2** and **3**). The results evidenced that all of the selected species have no interference in the detection of hydrazine. This result strongly indicated that probe **1** could be an excellent fluorescent probe towards hydrazine with strong anti-interference ability.

(Insert: Fig. 3)

3.7 Imaging of 1 to hydrazine in live cells

The intrinsic ability of probe **1** to target lysosome was investigated in living HeLa cells after addition of hydrazine (1.0×10^{-4}). The cells stained with probe **1** (1.0×10^{-5} M, 30 min, 25°C) were co-stained further with a commercially available lysosome-specific dye Neutral Red (Lysosome-Tracker) (1 mM, 30 min) in the culture medium. The imaging results show that the green image for the probe **1** channel obtained upon excitation at 457 nm is almost identical to the red image for the lysosome-Tracker channel obtained upon excitation at 640 nm (**Fig. 4**). The overlay between the fluorescence images of probe **1** and lysosome-Tracker discloses a Pearson's correlation coefficient of 0.82, suggesting the ability of probe **1** to target lysosome.

The cytotoxicity of probe **1** toward HeLa cells was measured using the 3-(4,5-dimethylthiazol-2-yl)-2,5-diphenyltetrazolium bromide (MTT) assay to evaluate the potential application of probe **1** in live cell imaging. The cellular viability was estimated to be greater than 87% after 1 h at the concentration of 10^{-5} M for probe **1**, suggesting the low cytotoxicity of probe **1** (**Fig. 5a**). Practical applications of **1** in imaging live HeLa cells were investigated using confocal fluorescence microscopy with a 457 nm diode laser. The confocal fluorescence microscopy images are shown in Figures **5b** and **5c**. After incubation of HeLa cells with **1** (10^{-5} M) for 30 min at 37°C, no fluorescence was detected at green (525 ± 25 nm) channel in the cytoplasm. Following addition of hydrazine (1.0×10^{-4}), an obvious increase at the green channel was observed, suggesting the reaction of **1** to hydrazine.

(Insert: Fig. 4)

(Insert: Fig. 5)

4. Conclusion

A turn-on fluorescent hydrazine-probe was synthesized and demonstrated. This probe can not only quantitatively detect hydrazine in wide concentration range, but also exhibits good selectivity and anti-interference ability over other various species. The good location ability toward lysosome, the low cytotoxicity and the application for selective detection of hydrazine in living cells has been successfully demonstrated, which offered a designing approach for recognizing of hydrazine.

Acknowledgements

We are grateful for the financial supports from National Natural Science Foundation of China (21601158 and U1504203), special foundation for outstanding young teachers of Zhengzhou University.

References

- [1] Sanabria-Chinchilla J, Asazawa K, Sakamoto T, Yamada K, Tanaka H, Strasser P. Noble Metal-Free Hydrazine Fuel Cell Catalysts: EPOC Effect in Competing Chemical and Electrochemical Reaction Pathways. *J Am Chem Soc* 2011;133:5425–31.
- [2] Serov A, Padilla M, Roy AJ, Atanassov P, Sakamoto T, Asazawa K, Tanaka H: Anode Catalysts for Direct Hydrazine Fuel Cells: From Laboratory Test to an Electric Vehicle. *Angew Chem Int Ed* 2014;53: 10336–9.
- [3] Sakamoto T, Asazawa K, Sanabria-Chinchilla J, Martinez U, Halevi B, Atanassov P, Strasser P, Tanaka H. Combinatorial discovery of Ni-based binary and ternary catalysts for hydrazine electrooxidation for use in anion exchange membrane fuel cells. *J. Power Sources* 2014;247:605–11.
- [4] Sutton AD, Burrell AK, Dixon DA, Garner EB, Gordon JC, Nakagawa T, Ott KC, Robinson P, Vasiliu M. Regeneration of Ammonia Borane Spent Fuel by Direct Reaction with Hydrazine and Liquid Ammonia. *Science* 2011;331:1426–9.
- [5] Ahmad R, Tripathy N, Jung DUJ, Hahn YB. Highly sensitive hydrazine chemical sensor based on ZnO nanorods field-effect transistor. *Chem Commun* 2014;50:1890–3.
- [6] Garrod S, Bollard ME, Nichollst AW, Connor SC, Connelly J, Nicholson JK, Holmes E. Integrated metabonomic analysis of the multiorgan effects of hydrazine toxicity in the rat. *Chem Res Toxicol* 2005;18:115–22.
- [7] Zelnick SD, Mattie DR, Stepaniak PC: Occupational exposure to hydrazines.

- Treatment of acute central nervous system toxicity. *Aviat Space Environ Med* 2003;74:1285–91.
- [8] Qian Y, Lin J, Han LJ, Lin L, Zhu HL. A resorufin-based colorimetric and fluorescent probe for live-cell monitoring of hydrazine. *Biosens Bioelectron* 2014;58:282–6.
- [9] Umar A, Rahman MM, Kim SH, Hahn Y-B. Zinc oxide nanonail based chemical sensor for hydrazine detection. *Chem Commun* 2008:166–8.
- [10] Gionfriddo E, Naccarato A, Sindona G, Tagarelli A. Determination of hydrazine in drinking water: Development and multivariate optimization of a rapid and simple solid phase microextraction-gas chromatography-triple quadrupole mass spectrometry protocol. *Anal Chim Acta* 2014;835:37–45.
- [11] Oh J-A, Park J-H, Shin H-S. Sensitive determination of hydrazine in water by gas chromatography-mass spectrometry after derivatization with ortho-phthalaldehyde. *Anal Chim Acta* 2013;769:79–83.
- [12] Cui L, Jiang K, Liu DQ, Facchine KL. Simultaneous quantitation of trace level hydrazine and acetohydrazide in pharmaceuticals by benzaldehyde derivatization with sample 'matrix matching' followed by liquid chromatography-mass spectrometry. *J Chromatogr A* 2016;1462:73–9.
- [13] Kosyakov DS, Amosov AS, Ul'yanovskii NV, Ladesov AV, Khabarov YG, Shpigun OA. Spectrophotometric determination of hydrazine, methylhydrazine, and 1,1-dimethylhydrazine with preliminary derivatization by 5-nitro-2-furaldehyde. *J. Anal Chem* 2017;72:171–7.

- [14] Dutta G, Nagarajan S, Lapidus LJ, Lillehoj PB. Enzyme-free electrochemical immunosensor based on methylene blue and the electro-oxidation of hydrazine on Pt nanoparticles. *Biosens Bioelectron* 2017;92:372–7.
- [15] Gupta R, Rastogi PK, Ganesan V, Yadav DK, Sonkar PK. Gold nanoparticles decorated mesoporous silica microspheres: A proficient electrochemical sensing scaffold for hydrazine and nitrobenzene. *Sens Actuators B* 2017;239:970–8.
- [16] Harraz FA, Ismail AA, Al-Sayari SA, Al-Hajry A, Al-Assiri MS. Highly sensitive amperometric hydrazine sensor based on novel α -Fe₂O₃/crosslinked polyaniline nanocomposite modified glassy carbon electrode. *Sens Actuators B* 2016;234:573–82.
- [17] Wu J, Zhou T, Wang Q, Umar A. Morphology and chemical composition dependent synthesis and electrochemical properties of MnO₂-based nanostructures for efficient hydrazine detection. *Sens Actuators B* 2016;224:878–84.
- [18] Fang B, Zhang CH, Zhang W, Wang GF. A novel hydrazine electrochemical sensor based on a carbon nanotube-wired ZnO nanoflower-modified electrode. *Electrochim Acta* 2009;55:178–82.
- [19] Zhang H, Liu R, Liu J, Li L, Wang P, Yao SQ, Xu Z, Sun H. A minimalist fluorescent probe for differentiating Cys, Hcy and GSH in live cells. *Chem Sci* 2016;7:256–60.
- [20] Chen H, Tang Y, Ren M, Lin W. Single near-infrared fluorescent probe with high- and low-sensitivity sites for sensing different concentration ranges of biological thiols with distinct modes of fluorescence signals. *Chem Sci* 2016;7:1896–903.

- [21] Tang Y, Kong X, Xu A, Dong B, Lin W. Development of a Two-Photon Fluorescent Probe for Imaging of Endogenous Formaldehyde in Living Tissues. *Angew Chem Int Ed* 2016;55:3356–9.
- [22] Xu W, Zeng Z, Jiang J-H, Chang Y-T, Yuan L. Discerning the Chemistry in Individual Organelles with Small-Molecule Fluorescent Probes. *Angew Chem Int Ed* 2016;55:13658–99.
- [23] Zhang R, Zhao J, Han G, Liu Z, Liu C, Zhang C, Liu B, Jiang C, Liu R, Zhao T, Han M-Y, Zhang Z. Real-Time Discrimination and Versatile Profiling of Spontaneous Reactive Oxygen Species in Living Organisms with a Single Fluorescent Probe. *J Am Chem Soc* 2016;138:3769–78.
- [24] Chen W, Pacheco A, Takano Y, Day JJ, Hanaoka K, Xian M. A Single Fluorescent Probe to Visualize Hydrogen Sulfide and Hydrogen Polysulfides with Different Fluorescence Signals. *Angew Chem Int Ed* 2016;55:9993–6.
- [25] Zhou W, Cao Y, Sui D, Lu C. Turn-On Luminescent Probes for the Real-Time Monitoring of Endogenous Hydroxyl Radicals in Living Cells. *Angew Chem Int Ed* 2016;55:4236–41.
- [26] Steiger AK, Pardue S, Kevil CG, Pluth MD. Self-Immolative Thiocarbamates Provide Access to Triggered H₂S Donors and Analyte Replacement Fluorescent Probes. *J Am Chem Soc* 2016;138:7256–9.
- [27] Wu X, Li L, Shi W, Gong Q, Ma H. Near-Infrared Fluorescent Probe with New Recognition Moiety for Specific Detection of Tyrosinase Activity: Design, Synthesis, and Application in Living Cells and Zebrafish. *Angew Chem Int Ed*

- 2016;55:14728–32.
- [28] Pinkert T, Furkert D, Korte T, Herrmann A, Arenz C. Amplification of a FRET Probe by Lipid-Water Partition for the Detection of Acid Sphingomyelinase in Live Cells. *Angew Chem Int Ed* 2017;56:2790–4.
- [29] Shao W, Chen G, Kuzmin A, Kutscher HL, Pliss A, Ohulchanskyy TY, Prasad PN: Tunable Narrow Band Emissions from Dye-Sensitized Core/Shell/Shell Nanocrystals in the Second Near-Infrared Biological Window. *J Am Chem Soc* 2016;138:16192–5.
- [30] Zhou DY, Wang YY, Jia J, Yu WZ, Qu BF, Li X, Sun X. H-Bonding and charging mediated aggregation and emission for fluorescence turn-on detection of hydrazine hydrate. *Chem Commun* 2015;51:10656–9.
- [31] Sun M, Guo J, Yang Q, Xiao N, Li Y. A new fluorescent and colorimetric sensor for hydrazine and its application in biological systems. *J Mater Chem B* 2014;2:1846–51.
- [32] Yu MM, Du WW, Zhou W, Li HX, Liu CX, Wei LH, Li ZX, Zhang HY. A 1,8-naphthalimide-based chemosensor with an off-on fluorescence and lifetime imaging response for intracellular Cr³⁺ and further for S₂. *Dyes Pigments* 2016;126:279–85.
- [33] Vijay K, Nandi C, Samant SD. Synthesis of a dihydroquinoline based merocyanine as a 'naked eye' and 'fluorogenic' sensor for hydrazine hydrate in aqueous medium and hydrazine gas. *RSC Adv* 2014;4:30712–7.
- [34] Reja SI, Gupta N, Bhalla V, Kaur D, Arora S, Kumar M. A charge transfer based

- ratiometric fluorescent probe for detection of hydrazine in aqueous medium and living cells. *Sens Actuators B* 2016;222:923–9.
- [35] He YY, Li ZX, Shi BJ, An Z, Yu MM, Wei LH, Ni ZH. A new near-infrared ratiometric fluorescent probe for hydrazine. *RSC Adv* 2017;7:25634–9.
- [36] Zhang JJ, Ning LL, Liu JT, Wang JX, Yu BF, Liu XY, Yao XJ, Zhang ZP, Zhang HX. Naked-Eye and Near-Infrared Fluorescence Probe for Hydrazine and Its Applications in In Vitro and In Vivo Bioimaging. *Anal Chem* 2015;87:9101–7.
- [37] Wang L, Liu FY, Liu HY, Dong YS, Liu TQ, Liu JF, Yao YW, Wan XJ. A novel pyrazoline-based fluorescent probe for detection of hydrazine in aqueous solution and gas state and its imaging in living cells. *Sens Actuators B* 2016;229:441–52.
- [38] Liu B, Liu Q, Shah M, Wang J, Zhang G, Pang Y. Fluorescence monitor of hydrazine in vivo by selective deprotection of flavonoid. *Sens Actuators B* 2014;202:194–200.
- [39] Li ZX, Zhang WY, Liu CX, Yu MM, Zhang HY, Guo L, Wei LH. A colorimetric and ratiometric fluorescent probe for hydrazine and its application in living cells with low dark toxicity. *Sens Actuators B* 2017;241:665–71.
- [40] Tang T, Chen YQ, Fu BS, He ZY, Xiao H, Wu F, Wang JQ, Wang SR, Zhou X. A novel resorufin based fluorescent "turn-on" probe for the selective detection of hydrazine and application in living cells. *Chin Chem Lett* 2016;27:540–4.
- [41] Yang Z, He Y, Lee JH, Park N, Suh M, Chae WS, Cao JF, Peng XJ, Jung H, Kang C, Kim JS. A Self-Calibrating Bipartite Viscosity Sensor for Mitochondria. *J Am Chem Soc* 2013;135:9181–5.

- [42] An Z, Li ZX, He YY, Shi BH, Wei LH, Yu MM. Ratiometric luminescence detection of hydrazine with a carbon dots–hemicyanine nanohybrid system RSC Adv 2017;7:10875–80.
- [43] Oushiki D, Kojima H, Terai T, Arita M, Hanaoka K, Urano Y, Nagano T. Development and Application of a Near-Infrared Fluorescence Probe for Oxidative Stress Based on Differential Reactivity of Linked Cyanine Dyes. J Am Chem Soc 2010;132:2795–801.
- [44] Fan JL, Sun W, Hu MM, Cao JF, Cheng GH, Dong HJ, Song KD, Liu YC, Sun SG, Peng XJ. An ICT-based ratiometric probe for hydrazine and its application in live cells. Chem Commun 2012;48:8117–9.
- [45] Oushiki D, Kojima H, Terai T, Arita M, Hanaoka K, Urano Y, Nagano T. Development and Application of a Near-Infrared Fluorescence Probe for Oxidative Stress Based on Differential Reactivity of Linked Cyanine Dyes. J Am Chem Soc 2010;132:2795–801.
- [46] Yu M, Du W, Li H, Zhang H, Li Z. Near-infrared ratiometric fluorescent detection of arginine in lysosome with a new hemicyanine derivative. Biosens Bioelectron 2017;92:385–9.
- [47] Zhao CC, Zhang XL, Li KB, Zhu SJ, Guo ZQ, Zhang LL, Wang FY, Fei Q, Luo SH, Shi P, Tian H, Zhu WH. Forster Resonance Energy Transfer Switchable Self-Assembled Micellar Nanoprobe: Ratiometric Fluorescent Trapping of Endogenous H₂S Generation via Fluvastatin-Stimulated Upregulation. J Am Chem Soc 2015;137:8490–8.

Figure Captions

Scheme 1 Synthesis of probe **1** and its recognition mechanism toward hydrazine.

Fig. 1. (a) Emission spectra of probe **1** (1.0×10^{-5} M, $V_{\text{HEPES}}:V_{\text{DMSO}} = 4:6$, pH = 7.40) upon titration of hydrazine (0–10.0 equiv to **1**) (b) The linearity of emission intensity at 517 nm with the concentration of hydrazine. (c) Kinetic curves of probe **1** (1.0×10^{-5} M, $V_{\text{HEPES}}:V_{\text{DMSO}} = 4:6$, pH = 7.40) at 517 nm with hydrazine at different concentrations [the concentrations of hydrazine are 0 M (black line), 4.0×10^{-6} M (red line), 8.0×10^{-6} M (green line), 1.2×10^{-5} M (blue line), and 1.6×10^{-5} M (cyan line)]. (d) Fluorescence change of **1** (1.0×10^{-5} M, $V_{\text{HEPES}}:V_{\text{DMSO}} = 4:6$, pH = 7.40) before (black line) and after (red line) addition of hydrazine (100 μ M) in different pH condition. The excitation wavelength was 440 nm and the reaction time was 1 h.

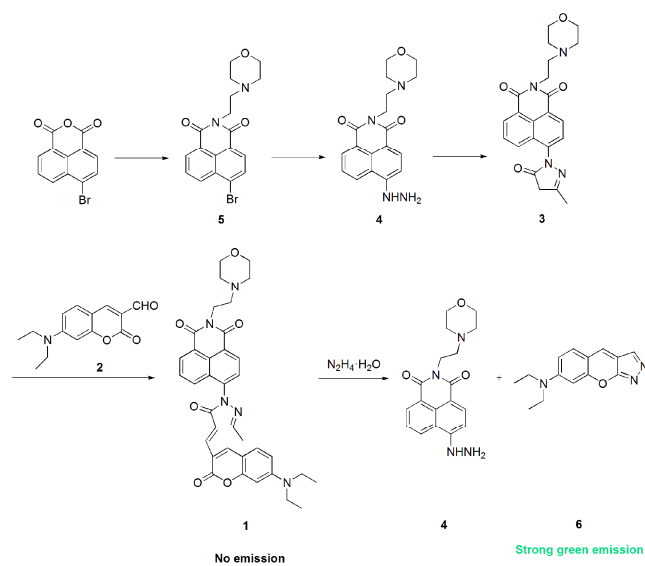
Fig. 2. Fluorescence responses of **1** (1.0×10^{-5} M, $V_{\text{HEPES}}:V_{\text{DMSO}} = 4:6$, pH=7.40) upon addition of different species (10 equiv of species relative to **1**) (red bars) and fluorescence changes of the mixture of **1** and hydrazine (1.0×10^{-4} M in water) after addition of an excess of the indicated species (10 equiv relative to **1**) (green bars) with excitation at 440 nm. The reaction time was 1 hour. I_{517} and I_0 represent the emission intensity at 517 nm after and before addition of hydrazine. The neutral molecules used were blank, Et_3N , $\text{NH}_3 \cdot \text{H}_2\text{O}$, $\text{C}_2\text{H}_4(\text{NH}_2)_2$, thiamine, urea, and Aniline. The metal ions used were blank, Na^+ , Mg^{2+} , Al^{3+} , K^+ , Ca^{2+} , Cr^{3+} , Mn^{2+} , Zn^{2+} , Pt^{2+} , and Pb^{2+} . The anions used were blank, HPO_4^{2-} , H_2PO_4^- , PO_4^{3-} , N_3^- , HSO_3^- , $\text{P}_2\text{O}_7^{4-}$, CO_3^{2-} , $\text{C}_2\text{O}_4^{2-}$, SiO_3^{2-} , Cl^- , F^- , NO_3^- , SO_3^{2-} , $\text{S}_2\text{O}_3^{2-}$, ClO_3^- , I^- , SO_4^{2-} , CH_3COO^- , and HS^- .

Fig. 3. Fluorescence responses of **1** (1.0×10^{-5} M, $V_{\text{HEPES}}:V_{\text{DMSO}} = 4:6$, pH = 7.40) upon addition of different species (10 equiv of species relative to **1**) (red bars) and fluorescence changes of the mixture of **1** and hydrazine (1.0×10^{-4} M in water) after

addition of an excess of the indicated species (10 equiv relative to **1**) (green bars) with excitation at 440 nm. The reaction time was 1 hour. I_{517} and I_0 represent the emission intensity at 517 nm after and before addition of hydrazine.

Fig. 4. (a), (b) Confocal fluorescence images of HeLa cells stained with probe **1** for 15 min (Channel 1: $\lambda_{\text{ex}}=457$ nm, $\lambda_{\text{em}}=525\pm 25$ nm, (a)) and Lysosome-Tracker (2.0 nm) for 15 min (Channel 2: $\lambda_{\text{ex}}=640$ nm, $\lambda_{\text{em}}=663-738$ nm, (b)). (c) Merged image of (a) and (b). (d) Bright-field image. (e) Intensity profile of regions of interest (ROIs) across HeLa cells. (f) Intensity Correlation plot of probe **1** and Lysosome-Tracker ($R_r = 0.82$).

Fig. 5. (a) Viability assay for HeLa cells treated with probe **1** in dark. Confocal fluorescence image in live HeLa cells contained by 10^{-5} M probe **1** (b) and cells of pretreated with 10^{-5} M probe **1** followed by incubation with 1.0×10^{-4} M hydrazine for 1 h (c). The excitation wavelength was 457 nm.



Scheme 1 Synthesis of probe **1** and its recognition mechanism toward hydrazine.

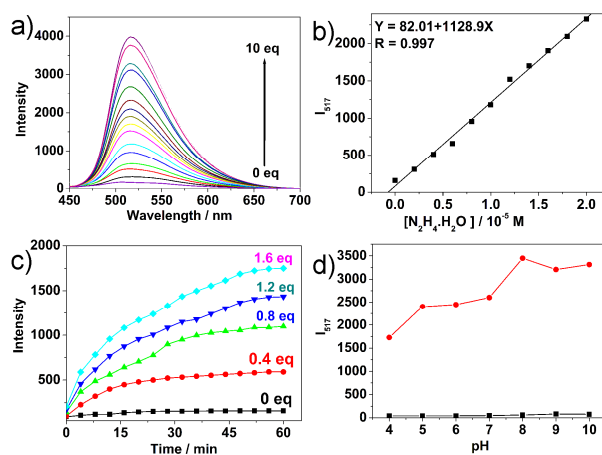


Fig. 1. (a) Emission spectra of probe **1** (1.0×10^{-5} M, $V_{\text{HEPES}}:V_{\text{DMSO}} = 4:6$, pH = 7.40) upon titration of hydrazine (0–10.0 equiv to **1**) (b) The linearity of emission intensity at 517 nm with the concentration of hydrazine. (c) Kinetic curves of probe **1** (1.0×10^{-5} M, $V_{\text{HEPES}}:V_{\text{DMSO}} = 4:6$, pH = 7.40) at 517 nm with hydrazine at different concentrations [the concentrations of hydrazine are 0 M (black line), 4.0×10^{-6} M (red line), 8.0×10^{-6} M (green line), 1.2×10^{-5} M (blue line), and 1.6×10^{-5} M (cyan line)]. (d) Fluorescence change of **1** (1.0×10^{-5} M, $V_{\text{HEPES}}:V_{\text{DMSO}} = 4:6$, pH = 7.40) before (black line) and after (red line) addition of hydrazine (100 μ M) in different pH condition. The excitation wavelength was 440 nm and the reaction time was 1 h.

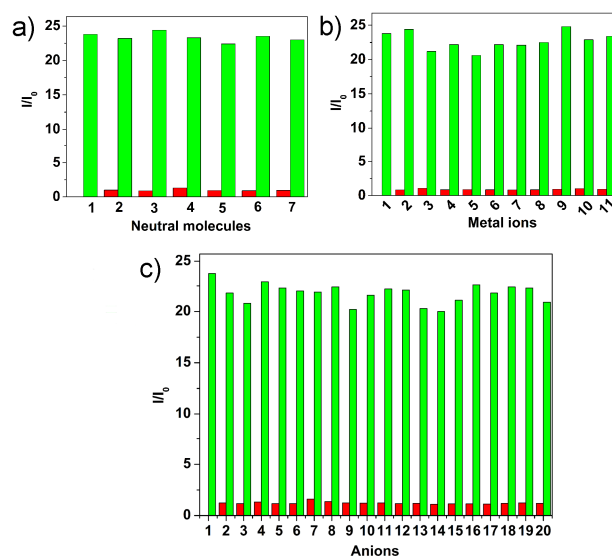


Fig. 2. Fluorescence responses of **1** (1.0×10^{-5} M, $V_{\text{HEPES}}:V_{\text{DMSO}}= 4:6$, pH=7.40) upon addition of different species (10 equiv of species relative to **1**) (red bars) and fluorescence changes of the mixture of **1** and hydrazine (1.0×10^{-4} M in water) after addition of an excess of the indicated species (10 equiv relative to **1**) (green bars) with excitation at 440 nm. The reaction time was 1 hour. I_{517} and I_0 represent the emission intensity at 517 nm after and before addition of hydrazine. The neutral molecules used were blank, Et_3N , $\text{NH}_3 \cdot \text{H}_2\text{O}$, $\text{C}_2\text{H}_4(\text{NH}_2)_2$, thiamine, urea, and Aniline. The metal ions used were blank, Na^+ , Mg^{2+} , Al^{3+} , K^+ , Ca^{2+} , Cr^{3+} , Mn^{2+} , Zn^{2+} , Pt^{2+} , and Pb^{2+} . The anions used were blank, HPO_4^{2-} , H_2PO_4^- , PO_4^{3-} , N_3^- , HSO_3^- , $\text{P}_2\text{O}_7^{4-}$, CO_3^{2-} , $\text{C}_2\text{O}_4^{2-}$, SiO_3^{2-} , Cl^- , F^- , NO_3^- , SO_3^{2-} , $\text{S}_2\text{O}_3^{2-}$, ClO_3^- , I^- , SO_4^{2-} , CH_3COO^- , and HS^- .

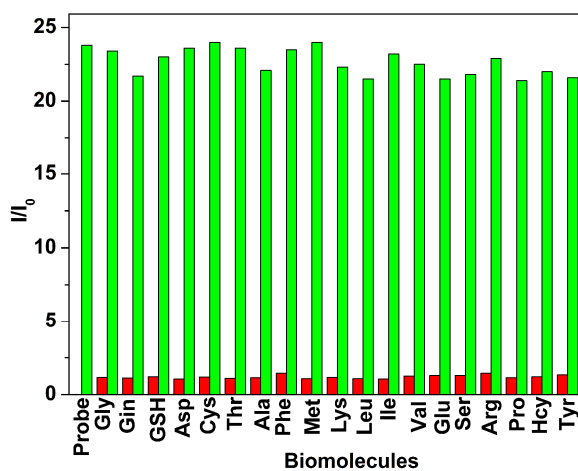


Fig. 3. Fluorescence responses of **1** (1.0×10^{-5} M, $V_{\text{HEPES}}:V_{\text{DMSO}} = 4:6$, pH = 7.40) upon addition of different species (10 equiv of species relative to **1**) (red bars) and fluorescence changes of the mixture of **1** and hydrazine (1.0×10^{-4} M in water) after addition of an excess of the indicated species (10 equiv relative to **1**) (green bars) with excitation at 440 nm. The reaction time was 1 hour. I_{517} and I_0 represent the emission intensity at 517 nm after and before addition of hydrazine.

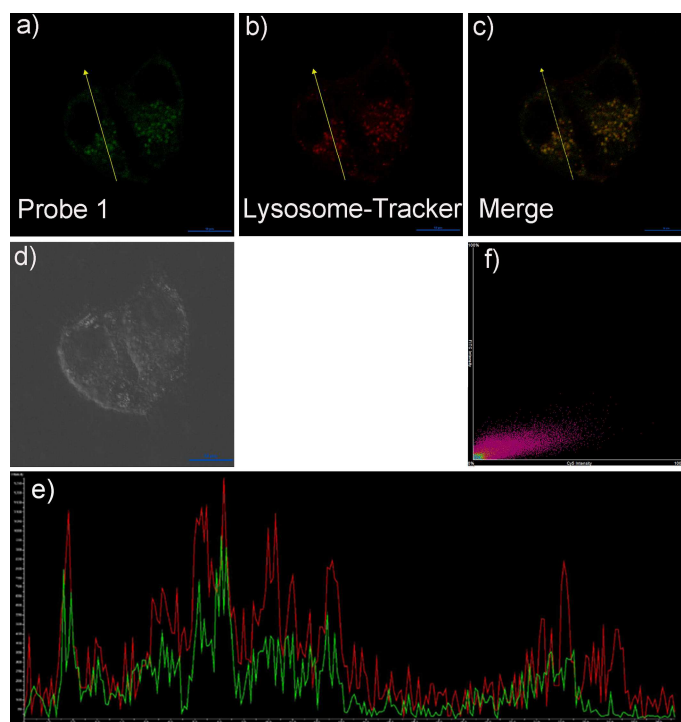


Fig. 4. (a), (b) Confocal fluorescence images of HeLa cells stained with probe **1** for 15 min (Channel 1: $\lambda_{\text{ex}}=457$ nm, $\lambda_{\text{em}}=525\pm 25$ nm nm, (a)) and Lysosome-Tracker (2.0 μm) for 15 min (Channel 2: $\lambda_{\text{ex}}=640$ nm, $\lambda_{\text{em}}=663-738$ nm, (b)). (c) Merged image of (a) and (b). (d) Bright-field image. (e) Intensity profile of regions of interest (ROIs) across HeLa cells. (f) Intensity Correlation plot of probe **1** and Lysosome-Tracker ($R_r = 0.82$).

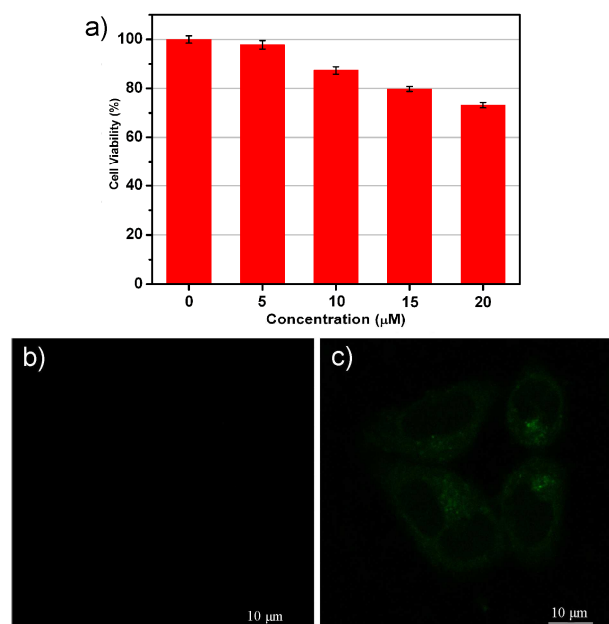


Fig. 5. (a) Viability assay for HeLa cells treated with probe **1** in dark. Confocal fluorescence image in live HeLa cells contained by 10^{-5} M probe **1** (b) and cells of pretreated with 10^{-5} M probe **1** followed by incubation with 1.0×10^{-4} M hydrazine for 1 h (c). The excitation wavelength was 457 nm.

Highlights

- ▶ A highly selective fluorescent probe for hydrazine shows off-on property.
- ▶ The probe can quantitatively detect hydrazine in the concentration range from 0 to 20 μM .
- ▶ The detection limit on fluorescence response of the probe can be as low as 140 nM.